Shear Band Direction in Amorphous Solids

- "An Atomistic Theory"

Ashwin J.

Institute for Plasma Research, Bhat Village, Gandhinagar-382428, India.

H.G.E Hentchel, O. Gendelman, C. Shor & I. Procaccia

January 2014

The Puzzle

"At high enough strains, amorphous solids undergo plastic failure via spontaneous strain localization along a shear band, the direction of which depends strongly on loading protocols."

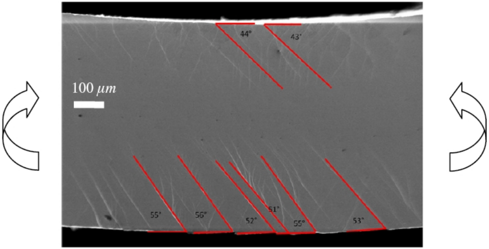

Bending experiment[1] on a plate of $Zr_{52.5}Al_{10}Ti_5Cu_{17.9}Ni_{14.6}$

[1] Y. F. Gao et al, Acta Materialia (59) 4159 (2011)

Plan of the talk

- Numerical simulations.
- Atomistic theory of plastic deformation.
- Comparison with simulations & experiments.
- Summary & road ahead.

Model glass former used

- Binary Lennard-Jones system:

$$U(r) = 4\epsilon_{\alpha\beta}\left[\left(\frac{\lambda_{\alpha\beta}}{r}\right)^{12} - \left(\frac{\lambda_{\alpha\beta}}{r}\right)^{6}\right]$$

$\epsilon_{\alpha\beta}$ and $\lambda_{\alpha\beta}$ are chosen for **quasi-crystalline**[1] ground state.

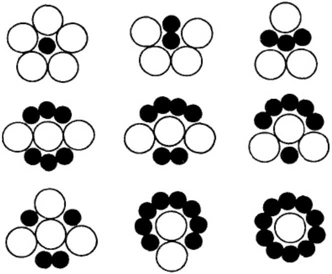

[1] M. Widom, K. J. Strandburg, and R. H. Swendsen, PRL (58), 706 (1987)

Cooling a liquid into glass

- Degree of disorder depends on cooling rate.

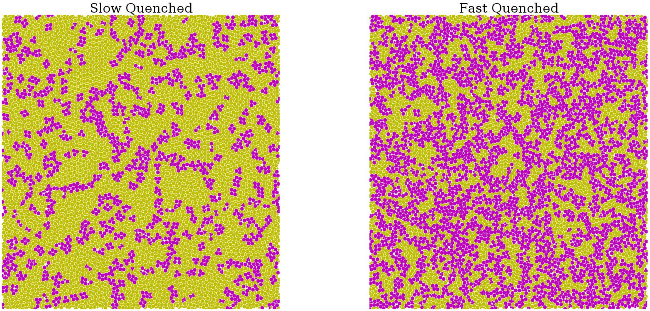

Motifs are colored **yellow** and defects colored **magenta**.

Cooling a liquid into glass

- Degree of disorder depends on cooling rate.

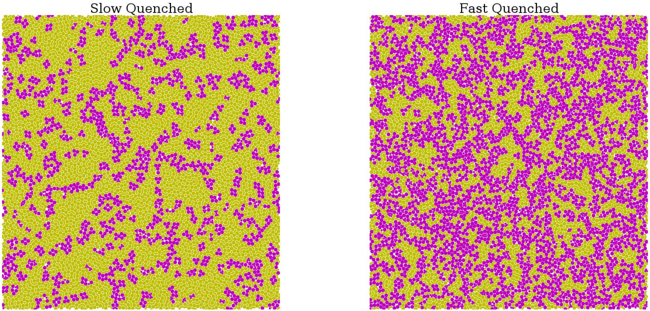

Motifs are colored **yellow** and defects colored **magenta**.

- Such **slow quenched** glasses deform via shear bands!

Deformation at zero temperature

- Take both athermal ($T \rightarrow 0$) & quasi-static ($\dot{\gamma} \rightarrow 0$) limits.

Deformation at zero temperature

- Take both athermal ($T \to 0$) & quasi-static ($\dot{\gamma} \to 0$) limits.
- From mechanical equilibrium, each particle moves as

$$\mathbf{r}_i^{new} = \mathbf{r}_i^{old} + \underbrace{\delta\gamma y_i^{old} \hat{x}}_{\text{affine step}}$$

Deformation at zero temperature

- Take both athermal ($T \to 0$) & quasi-static ($\dot{\gamma} \to 0$) limits.
- From mechanical equilibrium, each particle moves as

$$\mathbf{r}_i^{new} = \mathbf{r}_i^{old} + \underbrace{\delta\gamma y_i^{old} \hat{x}}_{\text{affine step}} + \underbrace{\mathbf{u}_i}_{\text{non-affine step}}$$

- $\mathbf{u}_i$ is necessary to restore equilibrium in amorphous materials.

Deformation at zero temperature

- Take both athermal ($T \to 0$) & quasi-static ($\dot{\gamma} \to 0$) limits.
- From mechanical equilibrium, each particle moves as

$$\mathbf{r}_i^{new} = \mathbf{r}_i^{old} + \underbrace{\delta\gamma y_i^{old}\hat{x}}_{\text{affine step}} + \underbrace{\mathbf{u}_i}_{\text{non-affine step}}$$

- $\mathbf{u}_i$ is necessary to restore equilibrium in amorphous materials.
- This also guarantees: $\underbrace{\mathbf{v}}_{\text{non-affine velocity}} = - \underbrace{\mathbf{H}^{-1}}_{\text{Inverse Hessian}} \cdot \underbrace{\mathbf{\Xi}}_{\text{affine force}}$

Elementary plastic instability

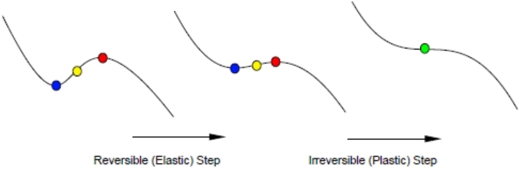

- At some $\gamma = \gamma_p$, a saddle point emerges.

Elementary plastic instability

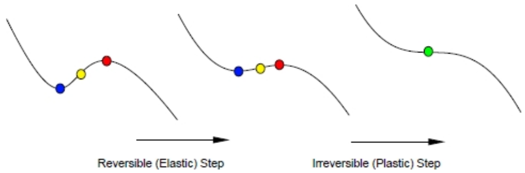

- At some $\gamma = \gamma_p$, a saddle point emerges.
- The lowest eigenvalue vanishes via: $\Lambda_p \sim \sqrt{\gamma_p - \gamma}$.
- Corresponding wave-function gets localized.

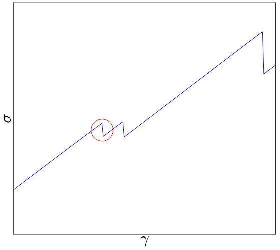

Elementary plastic instability

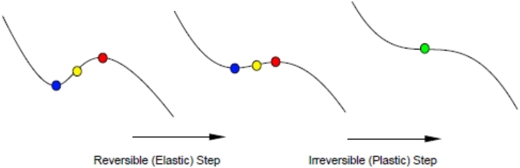

- At some $\gamma = \gamma_p$, a saddle point emerges.
- The lowest eigenvalue vanishes via: $\Lambda_p \sim \sqrt{\gamma_p - \gamma}$.
- Corresponding wave-function gets localized.

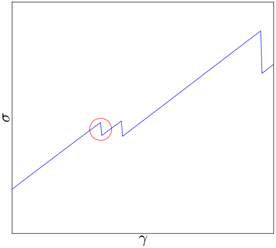

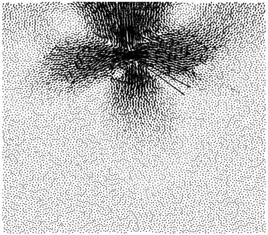

Elementary plastic instability

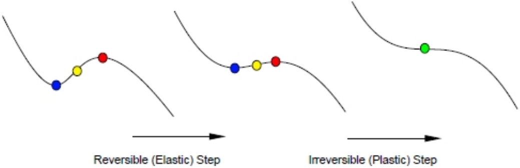

- At some $\gamma = \gamma_p$, a saddle point emerges.
- The lowest eigenvalue vanishes via: $\Lambda_p \sim \sqrt{\gamma_p - \gamma}$.
- Corresponding wave-function gets localized.

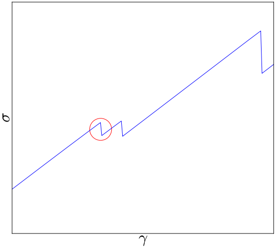

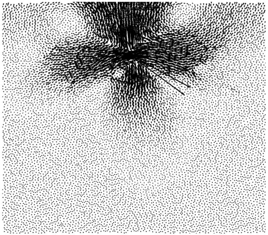

Uniaxial deformation

Instability

- Strain localizes into thin regions or shear bands.
- Angle θ w.r.t principal axis is higher in extension.

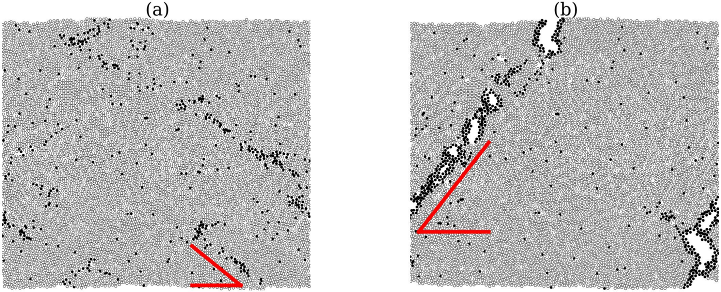

(a) Compression: $\theta = 46^o$ (b) Extension: $\theta = 54^o$

- Strain localizes into thin regions or shear bands.
- Angle θ w.r.t principal axis is higher in extension.

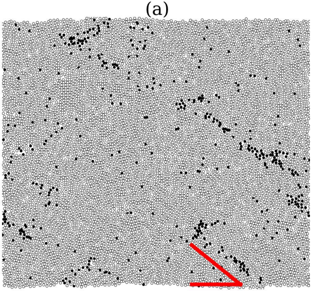

(a) Compression: $\theta = 46^o$

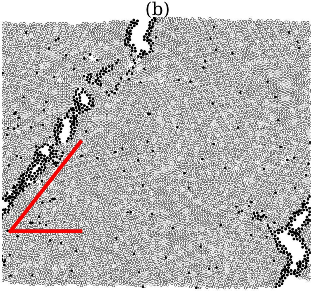

(b) Extension: $\theta = 54^o$

Next we will construct a theory for both these asymmetries.

Gedanken experiment of Eshelby (1957)

Elastic field due to an inclusion

Gedanken experiment of Eshelby (1957)

Elastic field due to an inclusion

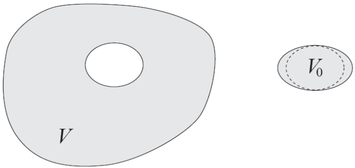

(1) Remove the inclusion from the matrix.

Gedanken experiment of Eshelby (1957)

Elastic field due to an inclusion

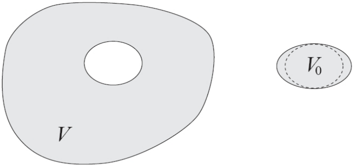

(1) Remove the inclusion from the matrix.

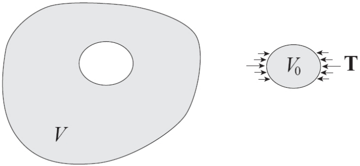

(2) Apply surface traction to make the inclusion return to its original shape.

Gedanken experiment of Eshelby (1957)

Elastic field due to an inclusion

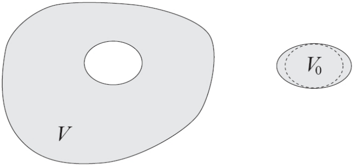

(1) Remove the inclusion from the matrix.

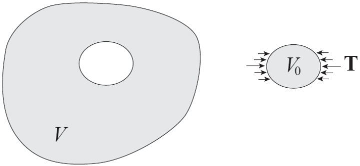

(2) Apply surface traction to make the inclusion return to its original shape.

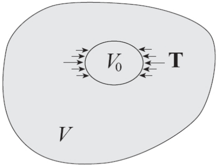

(3) Put the inclusion back into the matrix.

Gedanken experiment of Eshelby (1957)

Elastic field due to an inclusion

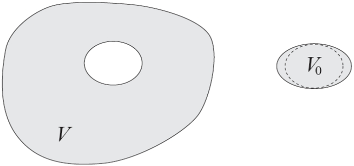

(1) Remove the inclusion from the matrix.

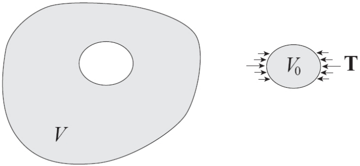

(2) Apply surface traction to make the inclusion return to its original shape.

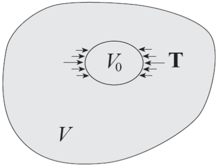

(3) Put the inclusion back into the matrix.

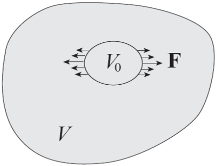

(4) Remove the traction T.

Characteristics of Eshelby inclusion

- Eigenstrain tensor

$$\epsilon^*_{\alpha\beta} = \zeta_n \hat{n}_\alpha \hat{n}_\beta + \zeta_k \hat{k}_\alpha \hat{k}_\beta$$

Characteristics of Eshelby inclusion

- Eigenstrain tensor

$$\epsilon^*_{\alpha\beta} = \zeta_n \hat{n}_\alpha \hat{n}_\beta + \zeta_k \hat{k}_\alpha \hat{k}_\beta$$

- $\epsilon^*_{\eta\eta} \neq 0$ as volume is allowed to change.

Characteristics of Eshelby inclusion

- Eigenstrain tensor

$$\epsilon^*_{\alpha\beta} = \zeta_n \hat{n}_\alpha \hat{n}_\beta + \zeta_k \hat{k}_\alpha \hat{k}_\beta$$

- $\epsilon^*_{\eta\eta} \neq 0$ as volume is allowed to change.
- In general, the ratio ζ_n/ζ_k depends on loading protocols.
- ζ_n/ζ_k uniquely determines the shear-band angle.

Mathematical procedure

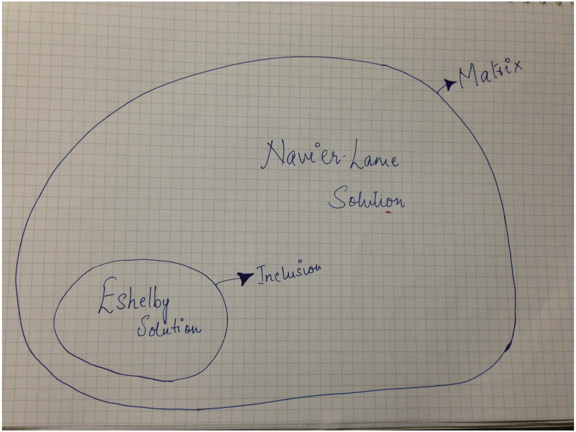

- Both solutions matched at the inclusion boundary:

$$\mathbf{u}^c(\mathbf{X}) \equiv \mathbf{u}^c(\zeta_n, \zeta_k, \lambda, \mu, a, \hat{\mathbf{n}}, \mathbf{X})$$

Energy contributions

To calculate the total energy we must calculate

$$E_{mat} = \frac{1}{2}\sigma^{\infty}_{\alpha\beta}\epsilon^{\infty}_{\beta\alpha}V$$ *"Energy of the strained matrix"*

$$E_{\infty} = -\frac{1}{2}\sigma^{\infty}_{\alpha\beta}\sum_{i=1}^{\mathcal{N}}\epsilon^{*,i}_{\beta\alpha}V_0^i$$ *"Energy of inclusions"*

$$E_{esh} = \frac{1}{2}\sum_{i=1}^{\mathcal{N}}(\sigma^{*,i}_{\alpha\beta} - \sigma^{c,i}_{\alpha\beta})\epsilon^{*,i}_{\beta\alpha}V_0^i$$ *"Self energy required to create the inclusions"*

$$E_{inc} = -\frac{1}{2}\sum_{i=1}^{\mathcal{N}}\epsilon^{*,i}_{\beta\alpha}V_0^i\sum_{j\neq i}\sigma^{c,j}_{\alpha\beta}(r^{ij})$$ *"Interaction energy between inclusions"*

Energy contributions

To calculate the total energy we must calculate

$$E_{mat} = \frac{1}{2}\sigma^{\infty}_{\alpha\beta}\epsilon^{\infty}_{\beta\alpha}V \quad \textit{"Energy of the strained matrix"}$$

$$E_{\infty} = -\frac{1}{2}\sigma^{\infty}_{\alpha\beta}\sum_{i=1}^{\mathcal{N}}\epsilon^{*,i}_{\beta\alpha}V^{i}_{0} \quad \textit{"Energy of inclusions"}$$

$$E_{esh} = \frac{1}{2}\sum_{i=1}^{\mathcal{N}}(\sigma^{*,i}_{\alpha\beta} - \sigma^{c,i}_{\alpha\beta})\epsilon^{*,i}_{\beta\alpha}V^{i}_{0} \quad \textit{"Self energy required to create the inclusions"}$$

$$E_{inc} = -\frac{1}{2}\sum_{i=1}^{\mathcal{N}}\epsilon^{*,i}_{\beta\alpha}V^{i}_{0}\sum_{j\neq i}\sigma^{c,j}_{\alpha\beta}(r^{ij}) \quad \textit{"Interaction energy between inclusions"}$$

The total energy of $\mathcal{N}$ such inclusions is thus

$$E = E_{mat} + E_{\infty} + E_{esh} + E_{inc}$$

Orientation of shear bands

Prediction requires minimizing energies

Orientation of shear bands

Prediction requires minimizing energies

- From $\frac{\partial E_\infty}{\partial \phi} = 0$, we get orientation of each inclusion

$$\phi = 0^o \quad \text{or} \quad \pi/2$$

Orientation of shear bands

Prediction requires minimizing energies

- From $\frac{\partial E_{\infty}}{\partial \phi} = 0$, we get orientation of each inclusion

$$\phi = 0^o \quad \text{or} \quad \pi/2$$

- Putting $\frac{\partial E_{inc}}{\partial \theta} = 0$, we find the shear band angle

$$\theta = \cos^{-1}\sqrt{\frac{1}{2} - \frac{1}{4}\frac{(\zeta_n + \zeta_k)}{(\zeta_n - \zeta_k)}}$$

Orientation of shear bands

Prediction requires minimizing energies

- From $\frac{\partial E_\infty}{\partial \phi} = 0$, we get orientation of each inclusion

$$\phi = 0^o \quad \text{or} \quad \pi/2$$

- Putting $\frac{\partial E_{inc}}{\partial \theta} = 0$, we find the shear band angle

$$\theta = \cos^{-1}\sqrt{\frac{1}{2} - \frac{1}{4}\frac{(\zeta_n + \zeta_k)}{(\zeta_n - \zeta_k)}}$$

- For volume conserving deformation such as pure shear

$$\theta = 45^o, \text{as} \quad \zeta_n = -\zeta_k$$

Orientation of shear bands

Prediction requires minimizing energies

- From $\frac{\partial E_\infty}{\partial \phi} = 0$, we get orientation of each inclusion

$$\phi = 0^o \quad \text{or} \quad \pi/2$$

- Putting $\frac{\partial E_{inc}}{\partial \theta} = 0$, we find the shear band angle

$$\theta = \cos^{-1}\sqrt{\frac{1}{2} - \frac{1}{4}\frac{(\zeta_n + \zeta_k)}{(\zeta_n - \zeta_k)}}$$

- For volume conserving deformation such as pure shear

$$\theta = 45^o, \text{as} \quad \zeta_n = -\zeta_k$$

- Any other loading condition **will realize a different angle!**

Calculating the angle

To calculate θ, we need the ratio ζ_n/ζ_k

(a) Compression

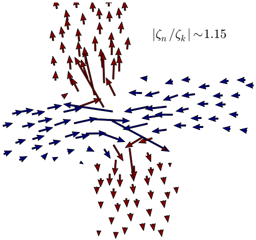

(b) Extension

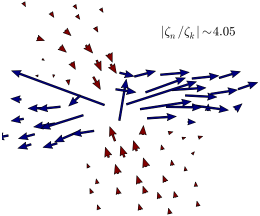

[1] **A J.**, O. Gendelman, I. Procaccia and C. Shor, PRE **(88)** 022310 (2013)

Calculating the angle

To calculate θ, we need the ratio ζ_n/ζ_k

(a) Compression

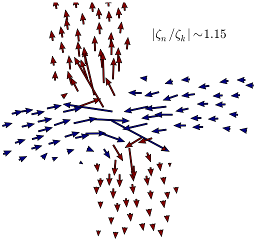

(b) Extension

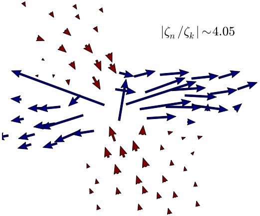

Plugging the observed values of ζ_n/ζ_k in the angle formula:

$$\theta \approx 46^0 \quad \text{for compression}$$

$$\theta \approx 54^0 \quad \text{for extension}$$

[1] **A J.**, O. Gendelman, I. Procaccia and C. Shor, PRE **(88)** 022310 (2013)

Limiting cases

Agreement with experiments

- The two limiting cases result from our prediction

$$\theta = 30^0 \quad \text{for the case} \quad |\zeta_n/\zeta_k| \to 0$$
$$\theta = 60^0 \quad \text{for the case} \quad |\zeta_n/\zeta_k| \to \infty$$

- Available experimental data conform to this prediction

	Poisson's ratio	Fracture or shear-band angle (compression)	Fracture or shear-band angle (tension)
$Pd_{40}Ni_{40}P_{20}$	0.403[12]	40.7–43.1[13], 42[14]	56[14]
$Pd_{77.5}Cu_{6}Si_{16.5}$	0.411[12]	–	51[15]
$Pd_{80}Si_{20}$	0.33[16]	–	54.7[17], 48–50[18]
$Zr_{40}Ti_{14}Ni_{10}Cu_{12}Be_{24}$	0.354[19]	42[19]	56[19]
$Zr_{40}Ti_{12}Ni_{9.4}Cu_{12.2}Be_{26.4}$	0.35–0.37	39.5–43.7[20], 40[21]	53.3–60.7[20], 50–59[21]
$Zr_{52.5}Al_{10}$ $Ni_{10}Cu_{15}Be_{12.5}$	0.35–0.37	-	55[22]
$Zr_{62}Ti_{10}Ni_{10}Cu_{14.5}Be_{3.5}$	0.35–0.37	39.5–43.7[23]	53.3–60.7[23]
$Zr_{63.2}$ $Ti_{9.9}Ni_{9.4}Cu_{13.4}Be_{4.1}$	0.35–0.37	39.4–41.4[21]	50–53[21]
$Zr_{52.5}Ni_{14.6}Al_{10}Cu_{17.9}Ti_{5}$	0.35–0.37	40–45[24], 44–46[25], 42[26]	55–56[24], 53–58,[25] 56[26]
$Zr_{54.5}$ $Ni_{8}Al_{10}Cu_{20}Ti_{7.5}$	0.35–0.37	42[26]	–
$Zr_{59}Ni_{8}Cu_{20}Al_{10}Ti_{3}$	0.35–0.37	42[27]	54[27], 54[26]
$Zr_{55}Ni_{5}Cu_{30}Al_{10}$	0.375[28]	40–43[26]	53–58[25]
$Zr_{60}Pd_{20}Cu_{20}$ Al_{10}	–	–	50[29]
$Zr_{65}Ni_{10}Al_{7.5}Cu_{7.5}Pd_{10}$	–	–	50[30]
$Cu_{60}Zr_{30}Ti_{10}$	~0.36	–	54[31]
$Ni_{78}Si_{10}B_{12}$	–	–	50–55[32]
$Cu_{60}Zr_{20}Hf_{10}Ti_{10}$	0.368[2]	40.5[33]	–
$Fe_{70}Ni_{10}B_{20}$	~0.35	–	60[34]
$Ni_{49}Fe_{29}P_{14}B_{6}Si_{2}$	0.37[35]	–	53[35]
$Co_{70}Si_{15}B_{10}Fe_{5}$	–	–	60[36]
$Co_{43}Fe_{20}Ta_{5.5}B_{31.5}$	–	44[37]	–
$Fe_{57.6}Co_{14.4}B_{19.2}Si_{4.8}Nb_{4}$	–	44[38]	–
$Al_{79.8}Y_{8.55}Ni_{4.75}Co_{1.9}Sc_{5}$	–	–	50[39]

Conclusions

- Shear band angle θ is **larger** in extension.

Conclusions

- Shear band angle θ is **larger** in extension.
- Our theory captures these asymmetries through the characteristics of Eshelby inclusions.

Conclusions

- Shear band angle θ is **larger** in extension.
- Our theory captures these asymmetries through the characteristics of Eshelby inclusions.
- Loading protocols which conserve volume lead to $\theta = 45^o$.
- Any other protocol will realize a different angle.

Conclusions

- Shear band angle θ is **larger** in extension.
- Our theory captures these asymmetries through the characteristics of Eshelby inclusions.
- Loading protocols which conserve volume lead to $\theta = 45^o$.
- Any other protocol will realize a different angle.
- In our theory θ is limited to lie between $30^o - 60^o$.
- Available experimental data conform to this prediction.

Future Work

- The present atomistic theory is valid in limits $\dot{\gamma} \to 0$, $T \to 0$.
- We would like to include:
  - finite temperature effects, $T \neq 0$.
  - finite strain rate effects, $\dot{\gamma} \neq 0$.

Thank You.